ThesisTitle

by

Daniel C. Cole

Other Degrees

A thesis submitted to the

Faculty of the Graduate School of the

University of Colorado in partial fulfillment

of the requirements for the degree of

Doctor of Philosophy

Physics Physics

2018

This thesis entitled:
ThesisTitle
written by Daniel C. Cole
has been approved for the Physics Physics

Reader1

Reader2

Date

The final copy of this thesis has been examined by the signatories, and we find that both the content and the form meet acceptable presentation standards of scholarly work in the above mentioned discipline.

Cole, Daniel C. (Ph.D., Physics)

ThesisTitle

Thesis directed by Dr. Scott A. Diddams

Optical frequency combs have revolutionized precision metrology by enabling measurements of optical frequencies, with implications both for fundamental scientific questions and for applications such as fast, broadband spectroscopy. In this thesis, I describe the development of comb generation platforms with smaller footprints and higher repetition rates, with the ultimate goal of bringing frequency combs to new applications in a chip-integrated package. I present two new types of frequency combs: electro-optic modulation (EOM) combs and Kerr-microresonator-based frequency combs (microcombs). First I describe the EOM comb scheme and, in particular, techniques for mitigating noise in the comb generation process, and I present the results of a proof-of-principle metrology experiment and some possible applications. Then I discuss developments in microcomb technology. I present novel 'soliton crystal' states, which have highly structured 'fingerprint' optical spectra that correspond to ordered pulse trains exhibiting crystallographic defects. These pulse trains arise through interaction of the solitons with avoided mode-crossings in the resonator spectrum. Next, I describe the direct and deterministic generation of single microresonator solitons using a phase-modulated pump laser. This technique removes the dependence on initial conditions that was formerly a universal feature of these experiments, presenting a solution to a significant technical barrier to the practical application of microcombs. I also discuss generation of Kerr combs in the Fabry-Perot (FP) geometry. I introduce a nonlinear partial differential equation describing dynamics in an FP cavity and discuss the differences between the FP geometry and the ring cavity, which is the geometry used in previous Kerr-comb experiments. Finally, I discuss a technique for reducing the repetition rate of a high-repetition-rate frequency comb, which will be a necessary post-processing step for some applications. I conclude with a discussion of avenues for future research, including the chip-integration of Fabry-Perot Kerr resonators and the use of band-engineered photonic crystal cavities to further simplify soliton generation.

Acknowledgements

The work in this thesis would not have been possible...

- Acknowledgement line 1
- Acknowledgement line 2

Contents

Figures

Chapter 1

PM Pumping

This chapter discusses the direct generation and control of single solitons in optical microring resonators using a pump-laser phase modulated at a frequency near the resonator's free spectral range. Based on a proposal by Taheri, Eftekhar, and Adibi in 2015 [42], these experimental results represent a promising new method for simple and deterministic generation of single solitons.

To illustrate the utility of using a phase-modulated pump laser, we first present theoretical investigations into the effect of this phase modulation (PM), and then we present experimental results on the generation and control of single solitons.

1.1 Theoretical investigation of soliton generation with a phase-modulated pump laser

To theoretically explore the physics of soliton generation with PM pumping, we use the LLE with a modified driving term that incorporates the effect of phase modulation [42]:

$$\frac{\partial\psi}{\partial\tau} = -(1+i\alpha)\psi + i|\psi|^2\psi - i\frac{\beta}{2}\frac{\partial^2\psi}{\partial\theta^2} + Fe^{i\delta_{PM}\cos\theta}. \tag{1.1}$$

Here δ_{PM} represents the phase-modulation index, where the resonator is driven by a field $E_{PM} = E_0 e^{i\delta_{PM}\cos(2\pi f_{PM} t)}$; $f_{PM} \sim f_{FSR}$ is the frequency of the applied phase modulation.

Simulations of Eq.1.1 reveal that PM transforms the resonator excitation spectrum from a series of $N = 0, 1, 2, ...$ up to N_{max} solitons to a single level $N = 1$ near threshold, eliminating degeneracy between these states as shown in Fig. 1.1. This occurs due to amplitude variations resulting from

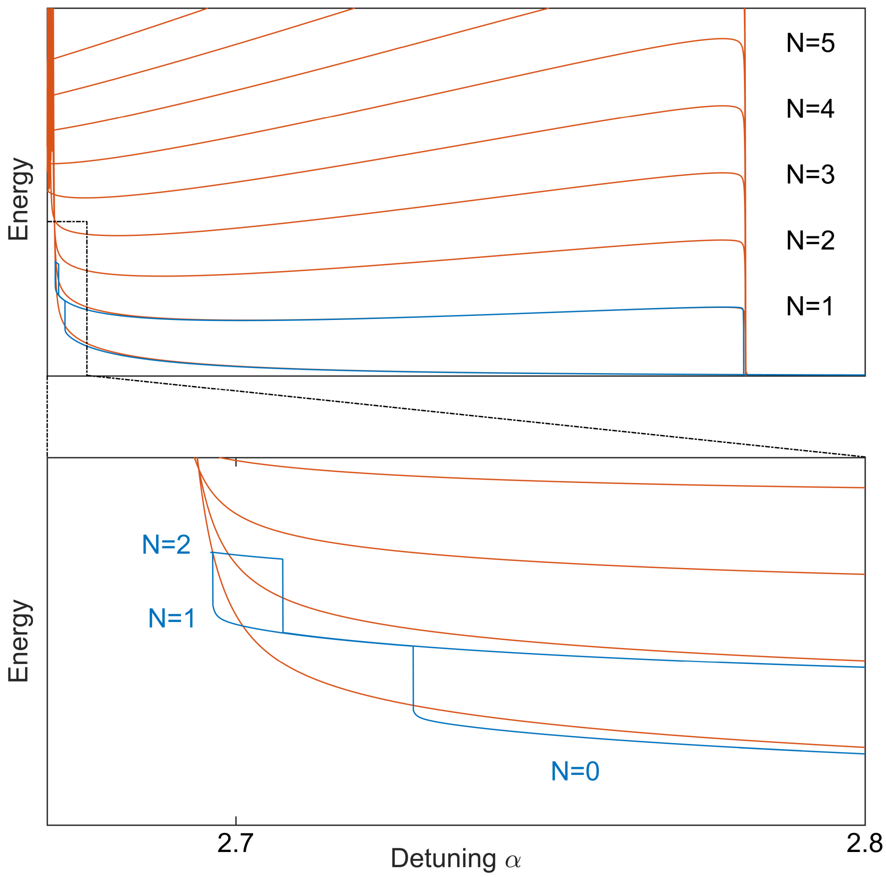

Figure 1.1: **title**text

the phase modulation, with dispersion and nonlinearity providing PM-to-AM conversion. We can gain some insight into the origin of this effect by inserting the ansatz $\psi(\theta,\tau) = \phi(\theta,\tau)e^{i\delta_{PM}\cos(\theta)}$ into Eq. 1.1 [40]. By expanding the second-derivative term and setting derivatives of ϕ to zero[1] we arrive at an equation for the quasi-CW background in the PM-pumped resonator:

$$F = (\gamma(\theta) + i\eta(\theta))\,\phi + i|\phi|^2\phi, \tag{1.2}$$

where effective local loss and detuning terms have been defined as:

$$\gamma(\theta) = 1 + \frac{\beta_2}{2}\delta_{PM}\cos\theta, \tag{1.3}$$

$$\eta(\theta) = \alpha - \frac{\beta_2}{2}\delta_{PM}^2\sin^2\theta. \tag{1.4}$$

[1] We note the contribution of Miro Erkintalo in suggesting this approximation.

This equation immediately yields an approximation for the stationary solution ψ_s:

$$\psi_s = \frac{Fe^{i\delta_{PM}\cos\theta}}{\gamma(\theta) + i\left(\eta(\theta) - \rho(\theta)\right)}, \tag{1.5}$$

where $\rho(\theta) = |\phi(\theta)|^2$ is the (smallest real) solution to the cubic polynomial that results from taking the modulus-square of Eq. 1.2:

$$F^2 = \left[\gamma(\theta)^2 + \left(\eta(\theta) - \rho(\theta)\right)^2\right]\rho(\theta). \tag{1.6}$$

In neglecting spatial derivatives of ϕ but retaining the derivatives of the phase term $e^{i\delta_{PM}\cos\theta}$ we have made the approximation that the dominant effect of dispersion comes from its action on the existing broadband phase-modulation spectrum. This model reveals that amplitude variations in the quasi-CW background can be expected as a result of the spatially-varying effective loss and detuning terms that arise from the periodically-chirped pump laser.

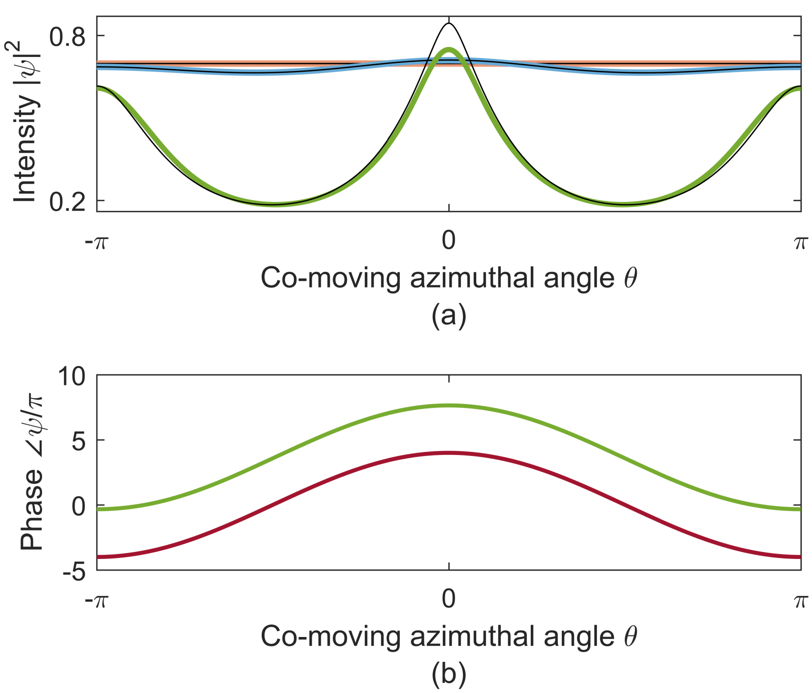

Figure 1.2: **title**text

Fig. 1.2 compares the predictions of numerical LLE simulations (color) with the analytical model (black). The two agree quantitatively at small modulation depth ($\delta_{PM} = \pi/2$, blue) and qualitatively at larger depth ($\delta_{PM} = 4\pi$, green). Both the simulations and the approximate analytic solution indicate that the background has two peaks per round trip in the presence of phase modulation, which suggests a mechanism for spontaneous single-soliton generation: At threshold the larger peak becomes locally unstable, and a soliton is formed by local modulation instability [41, 44]. Moreover, it is known that if solitons exist elsewhere they are pushed to the larger peak by the background's modulated phase [40]. This makes superpositions of $N > 1$ solitons unstable and practically forbidden. Generation of single solitons then simply requires tuning the pump power and frequency to appropriate values, regardless of initial conditions.

The detuning for soliton generation can be estimated using Eq. 1.2 by calculating the value of α where $\rho(\theta = 0) = 1$. This comes with a further approximation, as simulations reveal that the critical detuning for soliton formation is near but not necessarily at $\rho = 1$ because the spatial interval over which threshold is exceeded must have some minimum width. However, this approach quantitatively captures the behavior shown in Fig. 1.1, predicting soliton generation at $\alpha = 2.737$.

1.2 Spontaneous generation of single solitons using a phase-modulated pump laser

We demonstrate deterministic generation of single solitons without condensation from an extended pattern in a 22-GHz FSR silica ring resonator with $\Delta\nu \sim 1.5$ MHz linewidth [45]. We generate a frequency-agile laser for pumping the resonator by passing a CW laser through a single-sideband modulator that is driven by a voltage-controlled oscillator [46]; the seed laser is extinguished in the modulator and the resulting sideband can be swept by . The pump laser is phase-modulated with index $\delta_{PM} \sim \pi$ and amplified to normalized power F^2 between 2 and 6. We are able to measure and control the pump-laser detuning in real time using an AOM-shifted probe beam as shown in Fig. **??**, which allows thermal instabilities associated with the red detuning that is required for soliton generation to be overcome. The experimental setup and a frequency domain depiction of our locking scheme are shown in Fig. **??**.

rate and description here

To generate single solitons, we begin with large red detuning $\nu_0 - \nu_{pump}$ =40 MHz and decrease

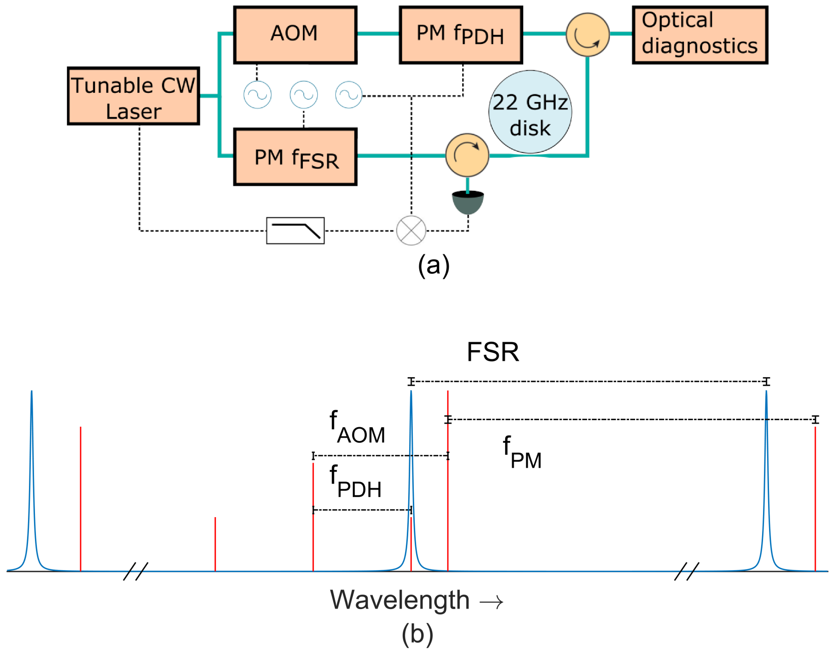

Figure 1.3: **title**text

the detuning until a soliton is generated near $\nu_0 - \nu_{pump}$ ~5 MHz detuning, where this value depends on the pump power and coupling condition. We measure the power converted by the Kerr nonlinearity to new frequencies by passing a portion of the resonator's output through an optical band-reject filter; this 'comb power' measurement reveals a step upon soliton formation, as shown in Fig. **??**. After soliton generation, we observe that the soliton can be preserved while the detuning is increased again up to a maximum value near , consistent with Fig. **??**. Additionally, we observe that it is possible to turn off the phase modulation without loss of the soliton, in agreement with the simulations presented in Ref. [42].

get from Jordan

Automating soliton generation by repeatedly scanning the laser into resonance ($\nu_0 - \nu_{pump}$ ~5 MHz) and back out again ($\nu_0 - \nu_{pump}$ ~20 MHz, far enough that the soliton is lost) has enabled reversible generation of 1000 solitons in 1000 trials over 100 seconds, with a measured 100 % success rate. Our probe beam allows measurement of the detuning at which soliton generation occurs, which changes little from run to run. We present a histogram of detuning measurements for the generation of 160 solitons in Fig. **??**.

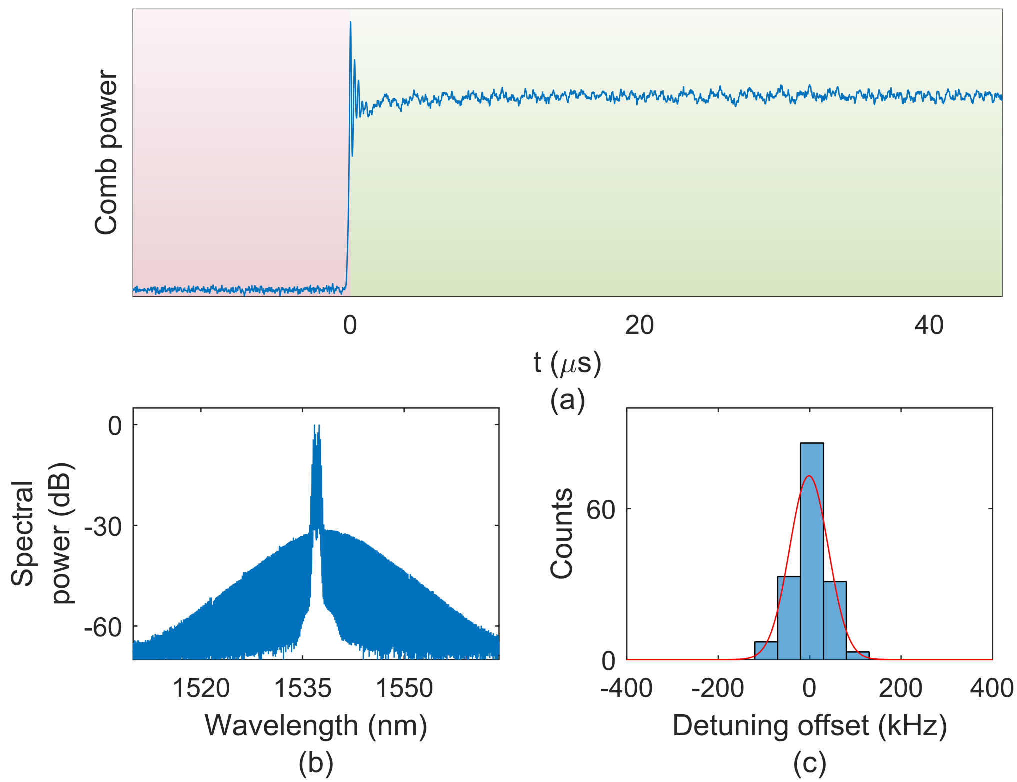

Figure 1.4: **title**text

1.3 Soliton control using a phase-modulated pump laser

In addition to enabling deterministic generation of single solitons, phase modulation of the pump laser also facilitates timing and repetition-rate control of the resulting pulse train. In our experiments, the repetition rate of the out-coupled pulse train (f_{rep}) remains locked to f_{PM} over a bandwidth of ±40 kHz. This observation is consistent with an estimate of the locking range $\delta_{PM} \times D_2/2\pi \sim$44 kHz that is presented in Ref. [40], where we have used the approximate value D_2 =14 kHz/mode. Fig. **??** shows the measured repetition rate as f_{PM} is swept sinusoidally through a range of ±50 kHz around the soliton's natural repetition rate; the repetition rate follows the PM except for glitches near the peaks of the sweep. In the inset of Fig. **??** we overlay the results of

LLE simulations that qualitatively match the observed behavior. These simulations are conducted by introducing the term $+\beta_1 \frac{\partial \psi}{\partial \theta}$ to the right-hand side of Eq. 1.1, where $\beta_1 = -2(f_{FSR} - f_{PM})/\Delta\nu$ incorporates a difference between the modulation frequency and the FSR of the resonator into the model; β_1 may be varied in time to simulate the sweep of f_{PM}. These simulations indicate that the periodic nature of the glitches is due to the residual pulling of the phase modulation on the soliton when the latter periodically cycles through the pump's phase maximum.

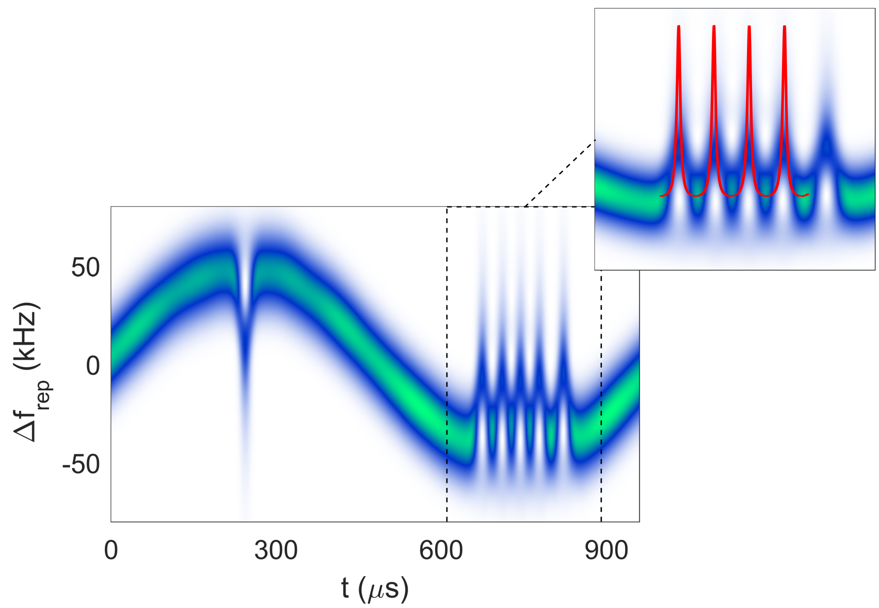

Figure 1.5: **title**text

To evaluate the utility of phase modulation for fast control of the soliton's properties, we measure the repetition rate of the pulse train as f_{PM} is rapidly switched ± 40 kHz, within the soliton's locking range. This measurement is conducted by photodetecting the pulse train after removing the central spectral lines corresponding to the spectrum of the pump laser using an optical band-reject filter. In order to obtain a measurement trace of the repetition rate as a function of time, the photodetected signal is split and one path is sent through a reactive circuit element that induces a frequency-dependent phase shift. By comparing the phase between the two paths as a function of time, the time-dependent repetition rate can be determined.

We construct eye-diagrams out of the resulting data; these are shown in Fig. **??**. In Fig. **??**,m

f_{PM} is switched with 200 μs period and 10 μs transition time; in Fig. **??** it is switched with 100 μs period and 60 ns transition time. These eye diagrams show that the PM enables exquisite control of the soliton pulse train.

We overlay a simulated eye diagram on the data in Fig. **??**. This simulation is conducted for parameters $\Delta\nu = 1.5$ MHz, $\delta_{PM} = 0.9\pi$ that are near the experimental values, and the agreement between measurement and simulation indicates that the measurements are consistent with fundamental LLE dynamics. Fig. **??** presents the results of additional LLE simulations; the basic result is that the switching speed of f_{rep} is limited by the resonator linewidth, and can be only modestly improved by increasing δ_{PM}.

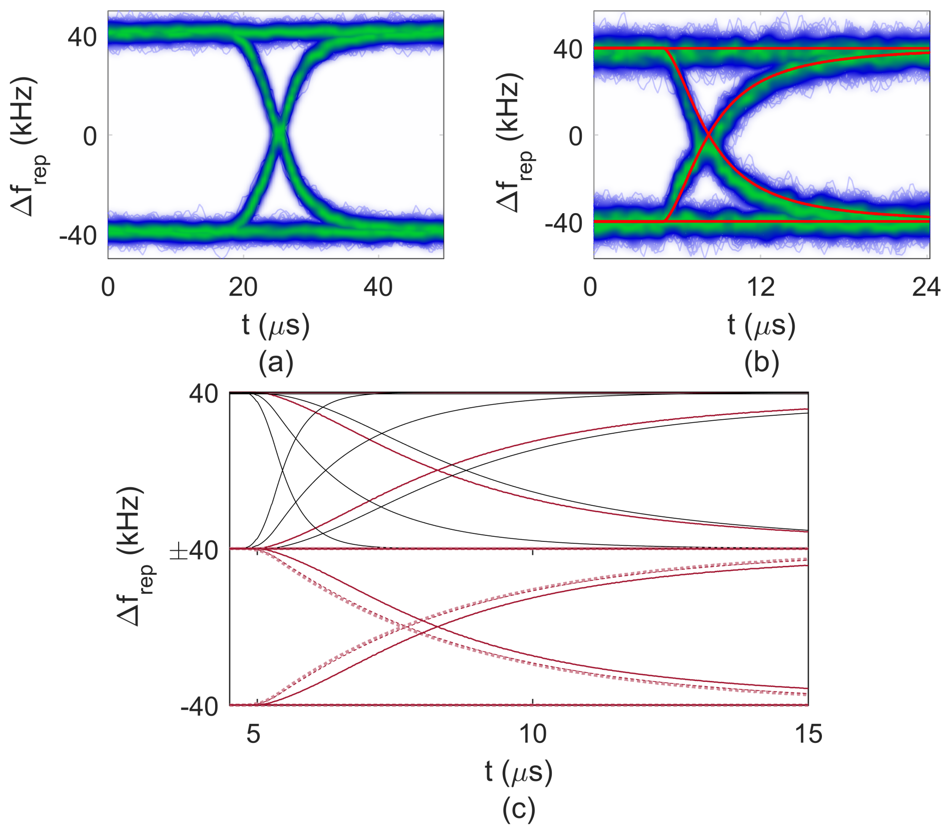

Figure 1.6: **title**text

1.4 Subharmonic phase modulation for high repetition-rate systems

One apparent barrier to the use of a phase-modulated pump laser for protected single-soliton generation and manipulation is the electronically-inaccessible FSRs of some typical microcomb resonators. However, it is possible to overcome this challenge by phase modulating at a subharmonic of the FSR. Simulations indicate that PM can directly excite single solitons with small modulation depth, e.g. $\delta_{PM} = 0.15\pi$. In this limit, only the first-order PM sidebands are relevant, and their amplitude and phase relative to the carrier control the dynamics. For a small desired modulation depth defined by the relationship between the first-order sidebands and the carrier, it is possible to modulate at a frequency $f_{mod} \sim f_{FSR}/N$ so that the N^{th}-order PM sidebands and the carrier address resonator modes with relative mode numbers -1, 0, and 1. The depth of modulation at the frequency f_{mod} can be chosen to fix the amplitudes of the N^{th}-order PM sidebands relative to the carrier and target a desired effective modulation depth. It is worth noting that when N is odd, phase modulation is recovered when the sidebands of order $-N$,0, and N address resonator modes -1, 0, and 1. When N is even the result is pure amplitude modulation, such that the driving term takes the form $F(1 + A\cos\theta)$. Simulations indicate that this AM profile also enables spontaneous single-soliton generation under some circumstances, but we note that this modulation profile cannot be obtained from a standard Mach-Zehnder modulator, which provides a drive like $F\cos(\eta+\delta\cos\theta)$.

Fig. **??** presents an example of this technique. We simulate spontaneous soliton generation with PM at $f_{mod} = f_{rep}/N = f_{rep}/21$. The effective modulation depth is 0.15π, which requires real modulation depth at the frequency f_{mod} with depth $\delta_{PM} \sim 8.3\pi$. Because the phase modulation spreads the optical power into the PM sidebands, use of this technique requires higher optical power for the same effective pumping strength; in this example the optical power must be increased by ∼15.6 dB. While the required modulation depth and pump power are higher with subharmonic phase modulation, neither is impractical. This technique could be used for spontaneous single-soliton generation in high-repetition rate systems; the example above indicates that it could be immediately applied in a 630 GHz-FSR resonator with 30 GHz phase modulation.

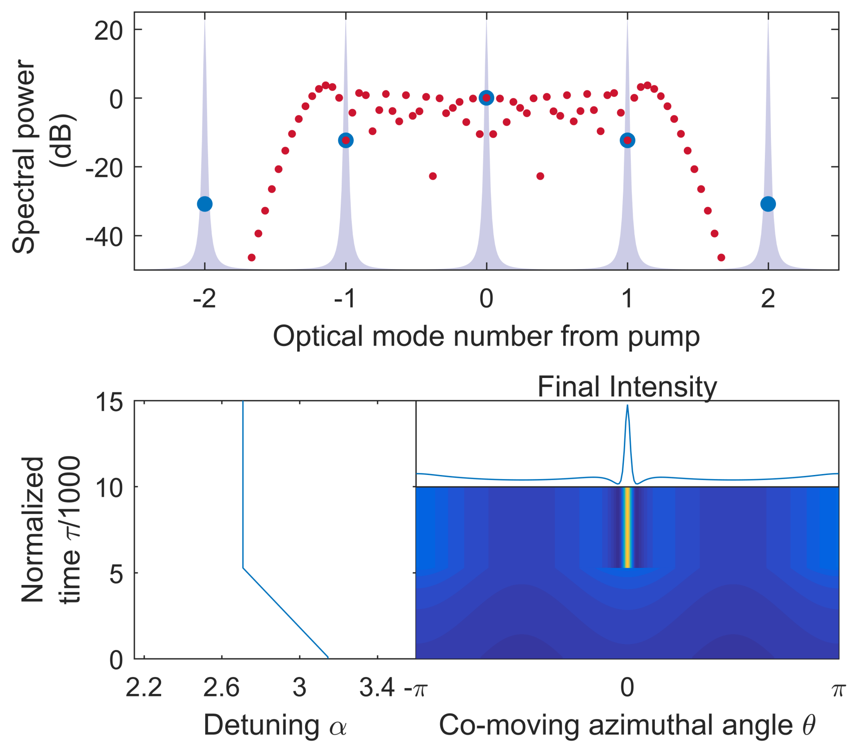

Figure 1.7: **title**text

References

[1] T. Udem, R Holzwarth, and T. W. Hänsch. Optical frequency metrology. *Nature*, 416 (6877), **2002**, 233–237. DOI: 10.1038/416233a.

[2] J. L. Hall. Nobel lecture: Defining and measuring optical frequencies. *Reviews of Modern Physics*, 78 (4), **2006**, 1279–1295. DOI: 10.1103/RevModPhys.78.1279.

[3] T. W. Hänsch. Nobel lecture: Passion for precision. *Reviews of Modern Physics*, 78 (4), **2006**, 1297–1309. DOI: 10.1103/RevModPhys.78.1297.

[4] J. K. Ranka, R. S. Windeler, and A. J. Stentz. Visible continuum generation in air–silica microstructure optical fibers with anomalous dispersion at 800 nm. *Optics Letters*, 25 (1), **2000**, 25. DOI: 10.1364/OL.25.000025.

[5] T. Steinmetz, T. Wilken, C. Araujo-Hauck, R. Holzwarth, T. W. Hänsch, L. Pasquini, A. Manescau, S. D'Odorico, M. T. Murphy, T. Kentischer, W. Schmidt, and T. Udem. Laser frequency combs for astronomical observations. *Science*, 321 (5894), **2008**, 1335–7. DOI: 10.1126/science.1161030.

[6] D. T. Spencer, T. Drake, T. C. Briles, J. Stone, L. C. Sinclair, C. Fredrick, Q. Li, D. Westly, B. R. Ilic, A. Bluestone, N. Volet, T. Komljenovic, L. Chang, S. H. Lee, D. Y. Oh, T. J. Kippenberg, E. Norberg, L. Theogarajan, M.-g. Suh, K. Y. Yang, H. P. Martin, K. Vahala, N. R. Newbury, K. Srinivasan, J. E. Bowers, S. A. Diddams, and S. B. Papp. An optical-frequency synthesizer using integrated photonics. *Nature*, 557, **2018**, 81–85. DOI: 10.1038/s41586-018-0065-7.

[7] R. W. Boyd. **Nonlinear Optics**. San Diego, CA: Elsevier, 2003.

[8] E. Obrzud, S. Lecomte, and T. Herr. Temporal solitons in microresonators driven by optical pulses. *Nature Photonics*, 11 (August), **2017**, 600–607. DOI: 10.1038/nphoton.2017.140. arXiv: 1612.08993.

[9] P. Del'Haye, S. A. Diddams, and S. B. Papp. Laser-machined ultra-high-Q microrod resonators for nonlinear optics. *Applied Physics Letters*, 102, **2013**, 221119.

[10] A. N. Oraevsky. Whispering-gallery waves. *Quantum Electronics*, 32 (42), **2002**, 377–400. DOI: 10.1070/QE2001v031n05ABEH002205. arXiv: arXiv:1011.1669v3.

[11] H. A. Haus. **Waves and Fields in Optoelectronics**. Englewood Cliffs: Prentice-Hall, 1984.

[12] S. M. Spillane, T. J. Kippenberg, O. J. Painter, and K. J. Vahala. Ideality in a Fiber-Taper-Coupled Microresonator System for Application to Cavity Quantum Electrodynamics. *Physical review letters*, 91 (4), **2003**, 043902. DOI: 10.1103/PhysRevLett.91.043902.

[13] V. S. Il'chenko and M. L. Gorodetskii. Thermal nonlinear effects in optical whispering gallery microresonators.pdf. *Laser Physics*, 2 (6), **1992**, 1004–1009.

[14] T. Carmon, L. Yang, and K. J. Vahala. Dynamical thermal behavior and thermal self-stability of microcavities. *Optics Express*, 12 (20), **2004**, 4742–4750. URL: http://www.ncbi.nlm.nih.gov/pubmed/19484026http://www.opticsinfobase.org/oe/abstract.cfm?uri=oe-12-20-4742.

[15] G. P. Agrawal. **Nonlinear Fiber Optics**. 4th. Burlington, MA: Elsevier, 2007.

[16] R. del Coso and J. Solis. Relation between nonlinear refractive index and third-order susceptibility in absorbing media. *Journal of the Optical Society of America B*, 21 (3), **2004**, 640. DOI: 10.1364/JOSAB.21.000640.

[17] P Del'Haye, A Schliesser, O Arcizet, T Wilken, R Holzwarth, and T. J. Kippenberg. Optical frequency comb generation from a monolithic microresonator. *Nature*, 450 (7173), **2007**, 1214–1217. DOI: 10.1038/nature06401.

[18] T. Kippenberg, S. Spillane, and K. Vahala. Kerr-Nonlinearity Optical Parametric Oscillation in an Ultrahigh-Q Toroid Microcavity. *Physical Review Letters*, 93 (8), **2004**, 083904. DOI: 10.1103/PhysRevLett.93.083904.

[19] A. A. Savchenkov, A. B. Matsko, D. Strekalov, M. Mohageg, V. S. Ilchenko, and L. Maleki. Low threshold optical oscillations in a whispering gallery mode CaF 2 resonator. *Physical Review Letters*, 93 (24), **2004**, 2–5. DOI: 10.1103/PhysRevLett.93.243905.

[20] I. H. Agha, Y. Okawachi, M. A. Foster, J. E. Sharping, and A. L. Gaeta. Four-wave-mixing parametric oscillations in dispersion-compensated high- Q silica microspheres. *Physical Review A - Atomic, Molecular, and Optical Physics*, 76 (4), **2007**, 1–4. DOI: 10.1103/PhysRevA.76.043837.

[21] F. Leo, S. Coen, P. Kockaert, S.-P. Gorza, P. Emplit, and M. Haelterman. Temporal cavity solitons in one-dimensional Kerr media as bits in an all-optical buffer. *Nature Photonics*, 4 (7), **2010**, 471–476. DOI: 10.1038/nphoton.2010.120.

[22] T. Herr, K. Hartinger, J. Riemensberger, C. Y. Wang, E. Gavartin, R. Holzwarth, M. L. Gorodetsky, and T. J. Kippenberg. Universal formation dynamics and noise of Kerr-frequency combs in microresonators. *Nature Photonics*, 6 (7), **2012**, 480–487. DOI: 10.1038/nphoton.2012.127.

[23] Y. K. Chembo and C. R. Menyuk. Spatiotemporal Lugiato-Lefever formalism for Kerr-comb generation in whispering-gallery-mode resonators. *Physical Review A*, 87, **2013**, 053852. DOI: 10.1103/PhysRevA.87.053852.

[24] S. Coen, H. G. Randle, T. Sylvestre, and M. Erkintalo. Modeling of octave-spanning Kerr frequency combs using a generalized mean-field Lugiato-Lefever model. *Optics letters*, 38 (1), **2013**, 37–39. URL: http://www.ncbi.nlm.nih.gov/pubmed/23282830.

[25] M. Haelterman, S. Trillo, and S. Wabnitz. Dissipative modulation instability in a nonlinear dispersive ring cavity. *Optics Communications*, 91 (5-6), **1992**, 401–407. DOI: 10.1016/0030-4018(92)90367-Z.

[26] T Hansson, M Bernard, and S Wabnitz. Modulational Instability of Nonlinear Polarization Mode Coupling in Microresonators. 35 (4), **2018**. URL: https://arxiv.org/pdf/1802.04535.pdf. arXiv: arXiv:1802.04535v1.

[27] T. Herr, V. Brasch, J. D. Jost, C. Y. Wang, N. M. Kondratiev, M. L. Gorodetsky, and T. J. Kippenberg. Temporal solitons in optical microresonators. *Nature Photonics*, 8 (2), **2014**, 145–152. DOI: 10.1109/CLEOE-IQEC.2013.6801769. arXiv: 1211.0733.

[28] Y. K. Chembo, I. S. Grudinin, and N Yu. Spatiotemporal dynamics of Kerr-Raman optical frequency combs. *Physical Review A*, 92 (4), **2015**, 4. DOI: 10.1103/PhysRevA.92.043818.

[29] C. Godey, I. V. Balakireva, A. Coillet, and Y. K. Chembo. Stability analysis of the spatiotemporal Lugiato-Lefever model for Kerr optical frequency combs in the anomalous and normal dispersion regimes. *Physical Review A*, 89 (6), **2014**, 063814. DOI: 10.1103/PhysRevA.89.063814.

[30] I. V. Barashenkov and Y. S. Smirnov. Existence and stability chart for the ac-driven, damped nonlinear Schrödinger solitons. *Physical Review E - Statistical Physics, Plasmas, Fluids, and Related Interdisciplinary Topics*, 54 (5), **1996**, 5707–5725. DOI: 10.1103/PhysRevE.54.5707.

[31] A Coillet and Y. K. Chembo. Routes to spatiotemporal chaos in Kerr optical frequency combs. *Chaos*, 24 (1), **2014**, 5. DOI: 10.1063/1.4863298. arXiv: arXiv:1401.0927v1.

[32] L. A. Lugiato and R Lefever. Spatial Dissipative Structures in Passive Optical Systems. *Physical Review Letters*, 58 (21), **1987**, 2209–2211.

[33] L. Lugiato and R Lefever. Diffraction stationary patterns in passive optical systems. *Interaction of Radiation with Matter*, **1987**.

[34] W. H. Renninger and P. T. Rakich. Closed-form solutions and scaling laws for Kerr frequency combs. *Scientific Reports*, 6 (1), **2016**, 24742. DOI: 10.1038/srep24742. arXiv: 1412.4164.

[35] X. Yi, Q.-F. Yang, K. Y. Yang, M.-G. Suh, and K. Vahala. Soliton frequency comb at microwave rates in a high-Q silica microresonator. *Optica*, 2 (12), **2015**, 1078–1085.

[36] S. Coen and M. Erkintalo. Universal scaling laws of Kerr frequency combs. *Optics letters*, 38 (11), **2013**, 1790–1792. DOI: 10.1364/OL.38.001790. arXiv: arXiv:1303.7078v1.

[37] V. Brasch, T. Herr, M. Geiselmann, G. Lihachev, M. H. P. Pfeiffer, M. L. Gorodetsky, and T. J. Kippenberg. Photonic chip-based optical frequency comb using soliton Cherenkov radiation. *Science*, 351 (6271), **2016**, 357. DOI: 10.1364/CLEO_SI.2015.STh4N.1. arXiv: 1410.8598.

[38] V. E. Lobanov, G. V. Lihachev, N. G. Pavlov, A. V. Cherenkov, T. J. Kippenberg, and M. L. Gorodetsky. Harmonization of chaos into a soliton in Kerr frequency combs. *Optics Express*, 24 (24), **2016**, 27382. DOI: 10.1126/science.aah4243. arXiv: 1607.08222.

[39] J. K. Jang, M. Erkintalo, S. G. Murdoch, and S. Coen. Writing and erasing of temporal cavity solitons by direct phase modulation of the cavity driving field. *Optics Letters*, 40 (20), **2015**, 4755–4758. DOI: 10.1364/OL.40.004755. arXiv: 1501.05289.

[40] J. K. Jang, M. Erkintalo, S. Coen, and S. G. Murdoch. Temporal tweezing of light through the trapping and manipulation of temporal cavity solitons. *Nature Communications*, 6, **2015**, 7370. DOI: 10.1038/ncomms8370. arXiv: 1410.4836 (cited on pages 2, 4, 6).

[41] Y. Wang, B. Garbin, F. Leo, S. Coen, M. Erkintalo, and S. G. Murdoch. Writing and Erasure of Temporal Cavity Solitons via Intensity Modulation of the Cavity Driving Field. *arXiv*, **2018**, 1802.07428. arXiv: 1802.07428 (cited on page 4).

[42] H. Taheri, A. A. Eftekhar, K. Wiesenfeld, and A. Adibi. Soliton formation in whispering-gallery-mode resonators via input phase modulation. *IEEE Photonics Journal*, 7 (2), **2015**, 2200309. DOI: 10.1109/JPHOT.2015.2416121 (cited on pages 1, 5).

[43] S. B. Papp, K. Beha, P. Del'Haye, F. Quinlan, H. Lee, K. J. Vahala, and S. A. Diddams. Microresonator frequency comb optical clock. *Optica*, 1 (1), **2014**, 10–14. DOI: 10.1364/OPTICA.1.000010. arXiv: 1309.3525.

[44] D Ceoldo, A Bendahmane, J Fatome, G Millot, T Hansson, D Modotto, S Wabnitz, and B Kilber. Multiple four-wave mixing and Kerr combs in a bichromatically pumped nonlinear fiber ring cavity. *Optics Letters*, 41 (23), **2016**, 5462–5465 (cited on page 4).

[45] H. Lee, T. Chen, J. Li, K. Y. Yang, S. Jeon, O. Painter, and K. J. Vahala. Chemically etched ultrahigh-Q wedge-resonator on a silicon chip. *Nature Photonics*, 6 (6), **2012**, 369–373. DOI: 10.1038/nphoton.2012.109. arXiv: 1112.2196 (cited on page 4).

[46] J. R. Stone, T. C. Briles, T. E. Drake, D. T. Spencer, D. R. Carlson, S. A. Diddams, and S. B. Papp. Thermal and Nonlinear Dissipative-Soliton Dynamics in Kerr Microresonator Frequency Combs. *arXiv*, **2017**, 1708.08405. URL: http://arxiv.org/abs/1708.08405. arXiv: 1708.08405 (cited on page 4).

[47] T. Kobayashi, T. Sueta, Y. Cho, and Y. Matsuo. High-repetition-rate optical pulse generator using a Fabry-Perot electro-optic modulator. *Applied Physics Letters*, 21 (8), **1972**, 341–343. DOI: 10.1063/1.1654403.

[48] M. Kourogi, K. Nakagawa, and M. Ohtsu. Wide-Span Optical Frequency Comb Generator for. 29 (10), **1993**.

[49] H. Murata, A. Morimoto, T. Kobayashi, and S. Yamamoto. Optical pulse generation by electrooptic-modulation method and its application to integrated ultrashort pulse generators. *IEEE Journal of Selected Topics in Quantum Electronics*, 6 (6), **2000**, 1325–1331. DOI: 10.1109/2944.902186.

[50] T. Sakamoto, T. Kawanishi, and M. Izutsu. frequency comb generation using a Mach – Zehnder. *Optics Letters*, 32 (11), **2007**, 1515–1517.

[51] I. Morohashi, T. Sakamoto, H. Sotobayashi, T. Kawanishi, I. Hosako, and M. Tsuchiya. Widely repetition-tunable 200 fs pulse source using a Mach-Zehnder-modulator-based flat comb generator and dispersion-flattened dispersion-decreasing fiber. *Optics letters*, 33 (11), **2008**, 1192–1194. DOI: 10.1364/OL.33.001192.

[52] A. Ishizawa, T. Nishikawa, A. Mizutori, H. Takara, S. Aozasa, A. Mori, H. Nakano, A. Takada, and M. Koga. Octave-spanning frequency comb generated by 250 fs pulse train emitted from 25 GHz externally phase-modulated laser diode for carrier-envelope-offset-locking. *Electronics Letters*, 46 (19), **2010**, 1343. DOI: 10.1049/el.2010.2228.

[53] R. Wu, V. R. Supradeepa, C. M. Long, D. E. Leaird, and A. M. Weiner. Generation of very flat optical frequency combs from continuous-wave lasers using cascaded intensity and phase modulators driven by tailored radio frequency waveforms. *Optics Letters*, 35 (19), **2010**, 3234. DOI: 10.1364/OL.35.003234. arXiv: 1005.5373.

[54] V. R. Supradeepa and A. M. Weiner. Bandwidth scaling and spectral flatness enhancement of optical frequency combs from phase-modulated continuous-wave lasers using cascaded four-wave mixing. *Optics Letters*, 37 (15), **2012**, 3066. DOI: 10.1364/OL.37.003066.

[55] A. J. Metcalf, V. Torres-company, D. E. Leaird, S. Member, A. M. Weiner, and A. Broadband. High-Power Broadly Tunable Electrooptic Frequency Comb Generator. *IEEE Journal of Selected Topics in Quantum Electronics*, 19 (6), **2013**, 3500306. URL: http://ieeexplore.ieee.org/stamp/stamp.jsp?arnumber=06553388.

[56] R. Wu, V. Torres-company, D. E. Leaird, and A. M. Weiner. Optical Frequency Comb Generation. 21 (5), **2013**, 6045–6052. DOI: 10.1364/OE.21.006045.

[57] J. M. Dudley, G. G. Genty, and S. Coen. Supercontinuum generation in photonic crystal fiber. *Reviews of Modern Physics*, 78 (4), **2006**, 1135–1184. DOI: 10.1103/RevModPhys.78.1135.

[58] A. M. Weiner. Femtosecond pulse shaping using spatial light modulators. *Review of Scientific Instruments*, 71 (5), **2000**, 1929–1960. DOI: 10.1063/1.1150614.

[59] K. Beha, D. C. Cole, P. Del'Haye, A. Coillet, S. A. Diddams, and S. B. Papp. Electronic synthesis of light. *Optica*, 4 (4), **2017**, 406–411. DOI: 10.1364/OPTICA.4.000406.

[60] a. a. Amorim, M. V. Tognetti, P Oliveira, J. L. Silva, L. M. Bernardo, F. X. Kärtner, and H. M. Crespo. Sub-two-cycle pulses by soliton self-compression in highly nonlinear photonic crystal fibers. *Optics letters*, 34 (24), **2009**, 3851–3853. DOI: 10.1364/OL.34.003851.

[61] S. Backus, C. G. Durfee, M. M. Murnane, and H. C. Kapteyn. High power ultrafast lasers. *Review of Scientific Instruments*, 69 (3), **1998**, 1207. DOI: 10.1063/1.1148795.

[62] A. Baltuska, M. Uiberacker, E. Goulielmakis, R. Kienberger, V. S. Yakovlev, T. Udem, T. W. Hänsch, and F. Krausz. Phase-Controlled Amplification of Few-Cycle Laser Pulses. *IEEE Journal of Selected Topics in Quantum Electronics*, 9 (4), **2003**, 972–989.

[63] C. Gohle, J. Rauschenberger, T. Fuji, T. Udem, A. Apolonski, F. Krausz, and T. W. Hänsch. Carrier envelope phase noise in stabilized amplifier systems. 30 (18), **2005**, 2487–2489.

[64] J. Rauschenberger, T. Fuji, M. Hentschel, A.-J. Verhoef, T. Udem, C. Gohle, T. W. Hänsch, and F. Krausz. Carrier-envelope phase-stabilized amplifier system. *Laser Physics Letters*, 3 (1), **2006**, 37–42. DOI: 10.1002/lapl.200510053.

[65] M. Hirano, T. Nakanishi, T. Okuno, and M. Onishi. Silica-Based Highly Nonlinear Fibers and Their Application. *Sel. Top. Quantum Electron.*, 15 (1), **2009**, 103–113. DOI: 10.1109/JSTQE.2008.2010241.

[66] D. Mandridis, I. Ozdur, F. Quinlan, M. Akbulut, J. J. Plant, P. W. Juodawlkis, and P. J. Delfyett. Low-noise, low repetition rate, semiconductor-based mode-locked laser source suitable for high bandwidth photonic analog – digital conversion. *Applied Optics*, 49 (15), **2010**, 2850–2857.

[67] D. C. Cole, K. M. Beha, S. A. Diddams, and S. B. Papp. Octave-spanning supercontinuum generation via microwave frequency multiplication. *Proceedings of the 8th Sympsion on Frequency Standards and Metrology 2015, Journal of Physics: Conference Series*, 723, **2016**, 012035. DOI: 10.1088/1742-6596/723/1/012035.

[68] A. M. Heidt. Efficient Adaptive Step Size Method for the Simulation of Supercontinuum Generation in Optical Fibers. *Journal of Lightwave Technology*, 27 (18), **2009**, 3984–3991.

[69] J. Hult. A Fourth-Order Runge-Kutta in the Interaction Picture Method for Simulating Supercontinuum Generation in Optical Fibers. *Journal of Lightwave Technology*, 25 (12), **2007**, 3770–3775. DOI: 10.1109/JLT.2007.909373.

[70] R. Driad, J. Rosenzweig, R. E. Makon, R. Lösch, V. Hurm, H. Walcher, and M. Schlechtweg. InP DHBT-Based IC Technology for 100-Gb / s Ethernet. *IEEE Trans. on Electron. Devices*, 58 (8), **2011**, 2604–2609.

[71] D. Ferenci, M. Grozing, M. Berroth, R. Makon, R. Driad, and J. Rosenzweig. A 25 GHz Analog Demultiplexer with a Novel Track and Hold Circuit for a 50 GS / s A / D-Conversion System in InP DHBT Technology. In: **Microwave Symposium Digest**. 2012, pp. 1–3.